Heat conduction in silicon thin films: Effect of microstructure

Lanhua Wei,[a] Mark Vaudin, Cheol Song Hwang,[b] and Grady White
Ceramics Division, National Institute of Standards and Technology, Gaithersburg, Maryland 20899

Jason Xu and Andrew J. Steckl
Nanoelectronics Laboratory, University of Cincinnati, Cincinnati, Ohio 45221

(Received 14 November 1994; accepted 21 April 1995)

A study was made of the thermal properties of low pressure chemical vapor deposition (LPCVD) silicon thin films with amorphous and polycrystalline microstructures, produced by varying the substrate temperature. Thermal diffusivity measurements were conducted using a thermal wave technique. The thermal diffusivity of the polycrystalline films was found to be about three times that of the amorphous films, but about one eighth that of bulk silicon single crystals. There was also an indication that the diffusivity increased with deposition temperature above the transition temperature from the amorphous to the polycrystalline state. The relationships between the thermal properties and microstructural features, such as grain size and grain boundary, are discussed.

I. INTRODUCTION

Silicon is the most important material in semiconductor technology and microelectronics systems. Silicon thin films, both amorphous and crystalline, are of great practical importance in device design.[1–3] In contrast to the extensive study of electronic, mechanical, and optical properties, little attention has been paid to the thermal properties of silicon films. Thermal properties of silicon films are potentially important not only for their scientific interest in relation to phonon scattering mechanisms, but also for practical reasons, as in advanced high-power devices. Because energy dissipation by local heating remains a critical limiting issue in device operation,[3,4] thermal conductivity of silicon films is a crucial performance and reliability factor in electronic circuits and integrated sensors.

Existing thermal property studies have focused almost exclusively on bulk single-crystal silicon. However, thin films can have complex microstructures,[5,6] which can lead to thermal properties different from those of the bulk.[7,8] Such differences and the related microstructural origins have not been well studied for silicon.

Measurement of thermal conductivities in thin film systems presents a special challenge to materials scientists and engineers. The major difficulty results from the very small thermal capacity of the film compared with that of the substrate, so that measurements tend to be insensitive to the presence of the film. With conventional contact probe techniques,[9,10] the accuracy is further compromised if the technique does not properly account for the thermal contact resistance between the probe and the film. It is in this context that thermal wave techniques,[11–14] with their noncontact configuration and capacity to probe local thermal properties, offer special advantages in thermal characterization of thin films.

We have investigated thermal conduction of silicon thin films using the photothermal deflection method, also known as the "mirage" thermal wave technique,[15,16] and have correlated these measurements with the film microstructures. The films were deposited by low pressure chemical vapor deposition (LPCVD) on fused quartz substrates at temperatures from 540 °C to 630 °C, with thicknesses on the order of 1 μm. Above a temperature of 570–580 °C, the films undergo a transition from the amorphous state to the polycrystalline state. In the polycrystalline state, the grain size and structure depend strongly on the substrate temperature during deposition. We show that the thermal diffusivity of the films is sensitive to crystallinity and microstructural features—the diffusivity of the polycrystalline state is about three times the diffusivity of the amorphous state, but only one eighth the diffusivity of the bulk single-crystal state. The study indicates that the film microstructure must be controlled in order to optimize thermal properties.

II. EXPERIMENTAL

A. Film preparation and microstructural characterization

Silicon thin films were deposited by LPCVD.[17] The substrates were commercial fused quartz plates, approximately 1 mm thick, with an average surface roughness less than 0.1 μm. After the substrates were degreased, the deposition process was carried out at

[a]Guest Scientist, on leave from Department of Physics and Astronomy, Wayne State University, Detroit, Michigan 48201.
[b]Guest Scientist, on leave from Department of Inorganic Materials Engineering, Seoul National University, Seoul, Korea.

66.7 Pa using silane at a flow rate of 25 sccm, with substrate temperatures ranging from 540 °C to 630 °C.

Film crystallinity was characterized by powder x-ray diffraction (XRD) using Cu K_α radiation. Scanning electron microscopy (SEM) was used to obtain information about surface morphology and to measure film thicknesses. We measured film thicknesses by fracturing the films and observing the cross sections using both secondary and backscattered electron imaging. Details of the film crystallinity and microstructure were examined by transmission electron microscopy (TEM), viewing the films in cross section. TEM specimens were prepared by face-to-face gluing of two thin cross sections, followed by grinding/polishing to 70 μm thickness, dimpling to 5 μm thickness, and ion milling to perforation.

B. Thermal wave technique

The apparatus for determining the thermal diffusivity of the silicon films by the thermal wave technique is shown schematically in Fig. 1.[18] An argon-ion laser beam, chopped by an acousto-optical modulator at frequencies between 10 and 60 kHz, is focused onto the film surface to provide a periodic localized heat source with a radius of about 6 μm. This generates periodic heat flow (thermal waves) in the silicon film/substrate system to a penetration depth of 2.5 to 5 μm, depending on the modulation frequency chosen for the heating laser beam. High frequencies are used here to shorten the thermal diffusion length, and hence to enhance the contribution of the film to the diffusivity measurement of the film/substrate system. Thermal waves are also generated in the air above the heated film surface; these waves are probed by a 30 μm diameter He–Ne laser beam that is reflected at a near-grazing incidence angle from the film surface near the heated spot. The thermal waves in the air are dominated by the thermal properties of the specimen because the heat capacity of a solid is much larger than that of air. The bouncing configuration of the probe laser beam[19] is adopted here so that the probe beam passes very close to the film in the area of the heating beam to maximize the detection sensitivity. The probe beam is refracted by the air as the index of refraction varies in time and space. The vector deflection (magnitude and phase) of both the normal and transverse components of the probe beam is monitored by a quad-cell detector. A microcomputer-controlled actuator-driven stage is then used to move the position of the heating beam across the probe beam, providing a thermal wave profile at a particular modulation frequency. The beam deflection is measured at each position of the actuator, and is thereby recorded as a function of heating beam position relative to the probe beam.

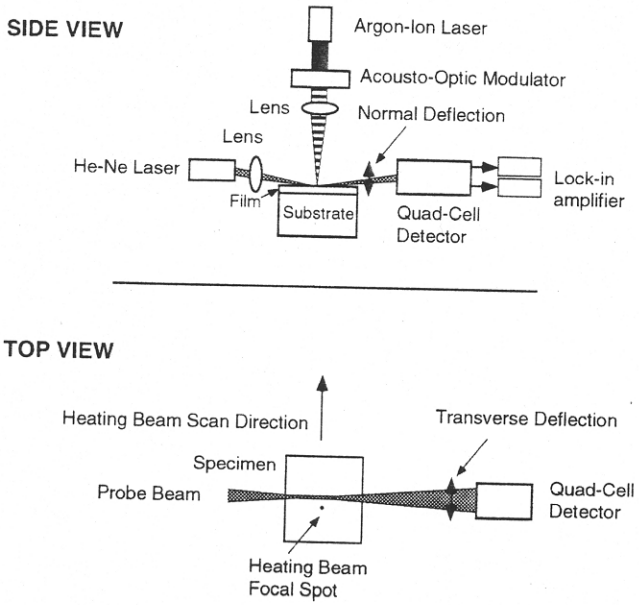

FIG. 1. Schematic diagram of the "mirage" thermal wave experimental setup for measuring diffusivity of thin films.

For thermal diffusivity evaluation, the scan is repeated at three frequencies, 10, 24, and 60 kHz. The resulting data set is analyzed by fitting it to a theoretical solution of a three-dimensional heat diffusion equation for an air/film/substrate system.[20] A typical data set consists of 3840 data points, including magnitude and phase of two vector components of the probe beam deflection for 320 stepped values of scan position and three modulation frequencies. The whole data set is fitted with a single set of fitting parameters, and the diffusivity of the film is obtained from a multiparameter, least-squares-fitting procedure.[20] The quality of the fit is measured by the statistical variance between the theory and experimental data. Documented thermal properties of the substrate[21] and independently measured beam geometry dimensions are used as input parameters.

Thermal diffusivity measurements are conducted at three or more randomly chosen surface spots for each thin film specimen, in order to average out any spatial nonuniformity. The diffusivities of an uncoated fused quartz substrate and a single crystal silicon wafer (1 mm thickness) are also measured to provide baselines for the measurements of the films.

III. RESULTS

A. Film microstructure characterization

Table I summarizes the microstructural data for the silicon thin films, obtained as described below.

Figure 2 shows XRD spectra for films deposited at temperatures from 570 °C to 630 °C, at intervals of 10 °C. No Bragg peaks are evident in the 570 °C spectrum, a result that is consistent with an amorphous structure. The spectrum from the 580 °C film contains a small 111 peak, indicating a small volume fraction of

TABLE I. Microstructure characterization data for the silicon thin films.

Deposition temperature (°C)	Crystallinity	Thickness (μm)	Area fraction of large grains (%)
540	Amorphous	3.6	N/A
550	Amorphous	3.3	N/A
560	Amorphous	2.1	N/A
570	Amorphous	2.5	N/A
580	Amorphous	2.0	N/A
590	Polycrystalline	1.6	0
600	Polycrystalline	0.8	15
610	Polycrystalline	1.1	13
620	Polycrystalline	0.7	13
630	Polycrystalline	1.0	36

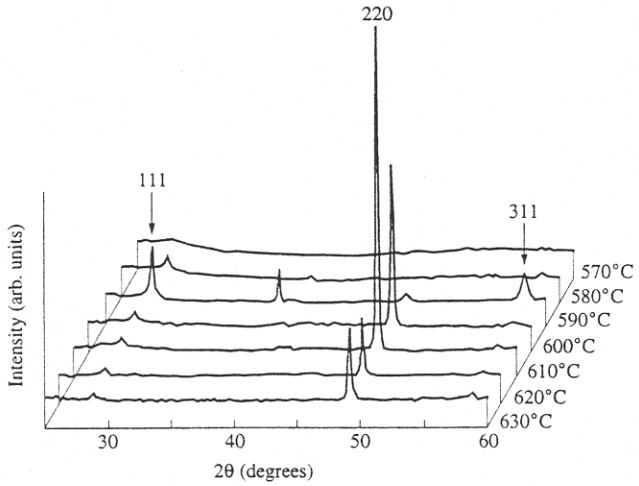

FIG. 2. X-ray diffraction spectra for films deposited between 570 °C and 630 °C.

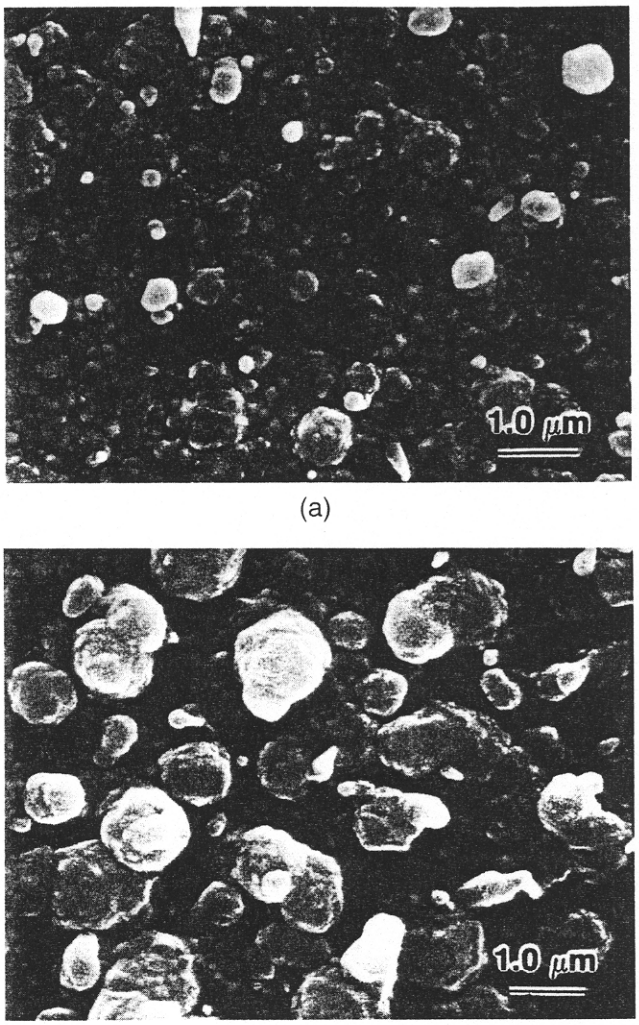

FIG. 3. SEM micrographs of polycrystalline silicon films, showing a change in surface morphology. (a) Specimen at deposition temperature of 620 °C. (b) Specimen at deposition temperature of 630 °C.

crystalline silicon in the film. At 590 °C and above, 111, 220, and 311 peaks appear, corresponding to a transition to the polycrystalline state. The intensities of the peaks are influenced by several variables: the volume fraction of crystalline material, which increases with increasing deposition temperature; the film thickness, which varies from film to film (see Table I); and the crystalline texture within the films, which changes from (111) at and below 590 °C to (110) above 600 °C. The 590 °C spectrum contains a peak at $2\theta = 39°$ which is as yet unexplained. In spite of the uncertainties regarding the interpretation of the relative intensities of the Bragg peaks, the phase transition occurring between 580 °C and 590 °C can be clearly observed in Fig. 2. The mean grain size for the polycrystalline films estimated from the peak line half-widths on the basis of the Scherrer formula[22] is about 60 nm.[17]

SEM micrographs reveal a progressive change in surface morphology of the polycrystalline films with increasing deposition temperature, from relatively smooth at 590 °C to coarse at 630 °C. The micrographs in Fig. 3 of the 620 °C and 630 °C films show this coarsening. Relatively large particles, on a scale of 1 μm, are observed on top of an otherwise fine surface structure. (Recall the 60 nm grain size from XRD above.) The size and area fraction of these larger particles are particularly enhanced for the specimen deposited at 630 °C. In order to evaluate quantitatively the fraction of these large particles, area fractions were measured for all the polycrystalline films. The SEM micrographs were scanned and digitized, and the area occupied by the particles was measured with an image analysis protocol. The area reaction of the large particles was then deduced for each polycrystalline film, and the results are listed in Table I. The thicknesses of the films, measured to within 5% in cross section by SEM (Sec. III. B), are also included in Table I.

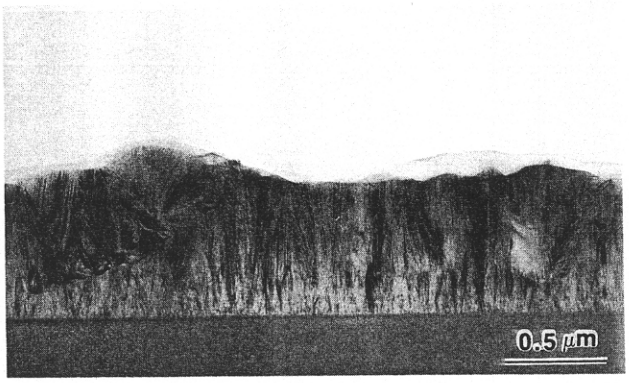

(a)

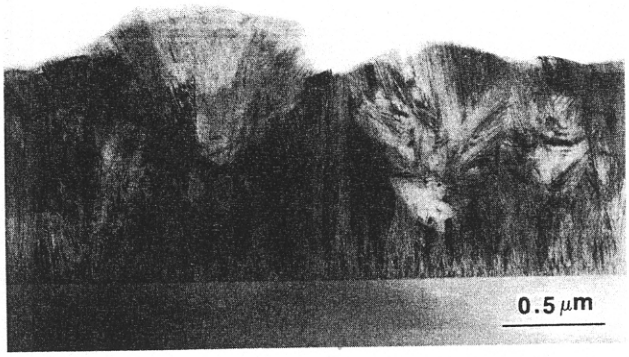

(b)

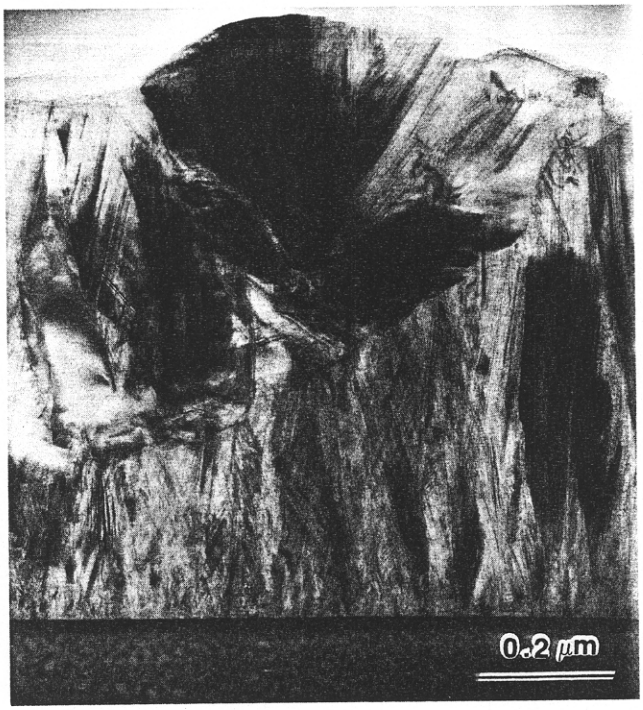

(c)

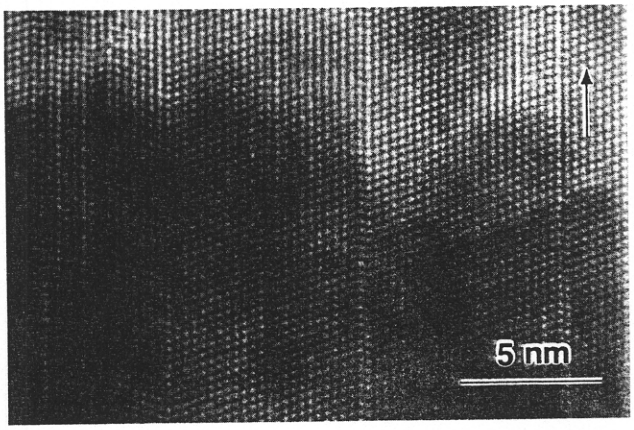

(d)

FIG. 4. TEM micrographs of cross sections of silicon thin films on fused quartz substrates. (a) Specimen at deposition temperature of 620 °C. (b) Specimen at deposition temperature of 630 °C. (c) A higher magnification micrograph of a large particle in (b). (d) A typical lattice-plane structure of the large particle shown in (c); the arrow indicates the film growth direction.

More detailed information on the microstructure of the polycrystalline films is available from the TEM micrographs. These micrographs reveal characteristic features of columnar growth[23] on smooth film/substrate interfaces. Figures 4(a) and 4(b) show cross-sectional micrographs of the polycrystalline films at 620 °C and 630 °C. Columnar growth features nearly normal to the substrate and the nucleation of large particles in the later stages of growth are evident. There are more such large particles in the 630 °C specimen [Fig. 4(b)] than in the 620 °C specimen [Fig. 4(a)], consistent with the SEM observations. Progressively magnified views of one large particle from Fig. 4(b) are shown in Figs. 4(c) and 4(d), and indicate that these particles consist of a number of highly twinned crystallites with clean twin boundaries, and that the average grain size in these particles is much larger than in the rest of the film. Figure 4(d) shows a representative impurity-free lattice-plane image of these large particles.

B. Film thermal diffusivity measurement

The thermal diffusivity was evaluated for each specimen with the thermal wave technique described above.

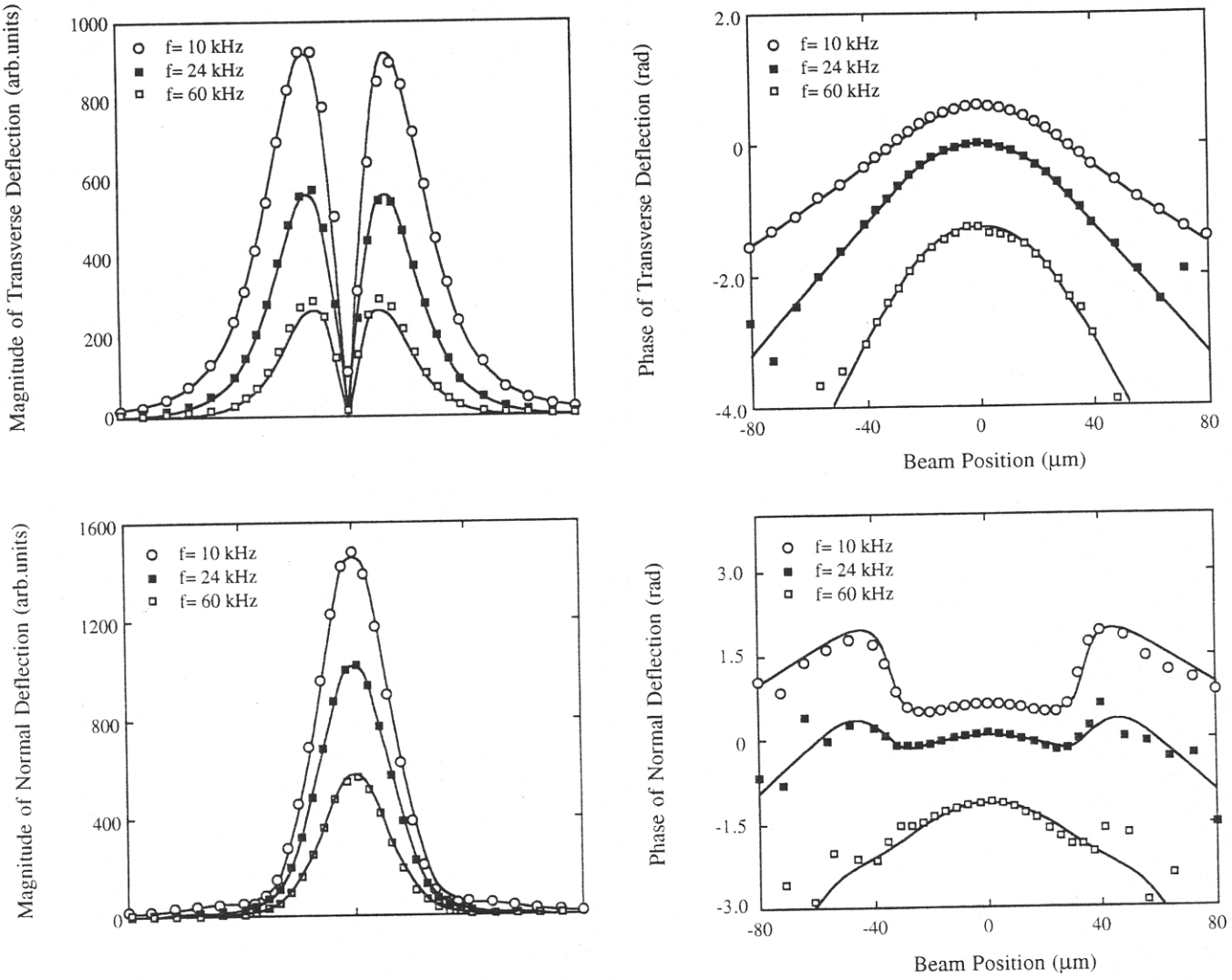

FIG. 5. Comparison of theory and experimental data of the magnitude and phase of both normal and transverse deflection signal for specimen at a deposition temperature of 610 °C, at three different frequencies. The symbols are experimental data and the solid curves are the theoretical fits.

Amplitudes and phases for both normal and transverse beam deflections at three modulation frequencies are shown in Fig. 5 for a specimen deposited at temperature 610 °C. The deflection components are plotted as a function of the distance between the heating and probe beams (see Fig. 1, top view). The space (x-axis) and time (inverse frequency) dependencies of the deflection data in Fig. 5 reflect the thermal properties of the materials. The theoretical fits (solid curves) to the experimental data (symbols) agree well within the scatter, with a variance 0.0006 (Sec. II. B). Because the thermal diffusivity of the substrate (0.007 cm^2/s) is small relative to that of the films (0.03–0.14 cm^2/s), the heat diffusion is primarily in-plane, so that it is the lateral diffusivity we are measuring here.

We emphasize the sensitivity of the measurement to changes in film diffusivity. Particularly sensitive is the phase of the normal deflection component. Figure 6 is a plot of this component for three representative specimens, uncoated fused quartz (substrate material), amorphous silicon film on fused quartz (deposition temperature 550 °C), and polycrystalline silicon film on fused quartz (deposition temperature 610 °C), at a frequency of 10 kHz. The distinct differences between the data from the three specimens reflect both differences in heat diffusion rates of the films and thermal property mismatches at the film/substrate interfaces.

The thermal diffusivity results for the silicon films are summarized in Fig. 7, as a function of deposition temperature; the data point positions are mean values and the bar lengths are the standard deviations. The measured diffusivity of single-crystal silicon is shown for comparison as the upper dashed line. The value 0.900 ± 0.05 cm^2/s agrees with a literature value 0.930 cm^2/s[21]

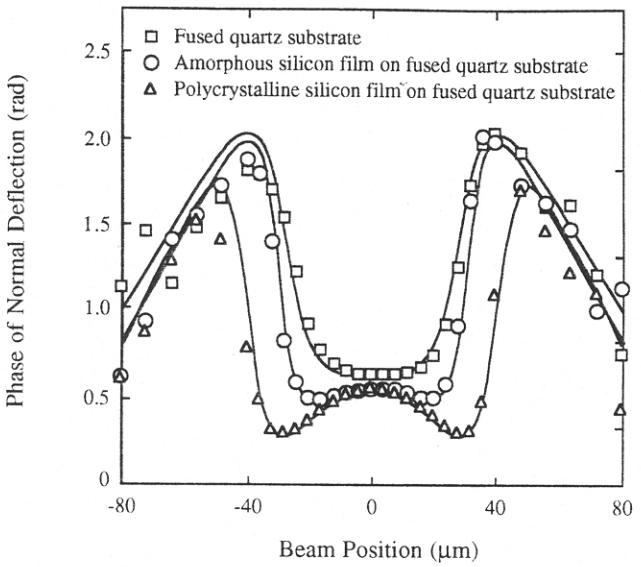

FIG. 6. Comparison of theory and experimental data of the phase of normal deflection signal for three representative specimens (at frequency of 10 kHz), uncoated fused quartz (substrate material), amorphous silicon film on fused quartz (deposition temperature 550 °C), and polycrystalline silicon on fused quartz (610 °C).

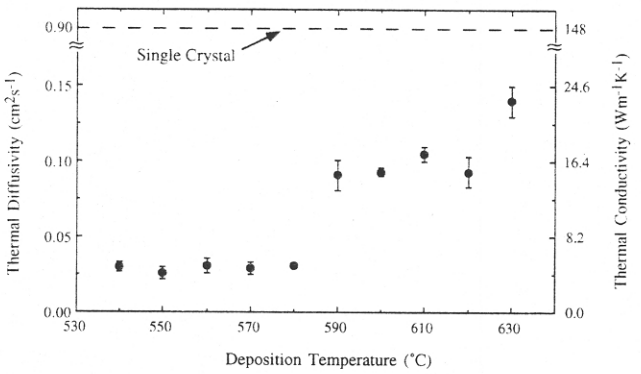

FIG. 7. Thermal diffusivity measurement results for the silicon thin films and a single-crystal silicon wafer. The film data are presented as a function of deposition temperature.

within the uncertainty. The thermal conductivity κ on the right-side axis is obtained from diffusivity using the definition

$$\alpha = \kappa/\rho c , \qquad (1)$$

where α is the thermal diffusivity, ρ the mass density, and c the specific heat. In the absence of any observed porosity in our films, we take $\rho c = 1.64\ \mathrm{J\,cm^{-3}\,K^{-1}}$ based on literature values for bulk single crystal silicon.[21]

The data in Fig. 7 divide into three distinct levels, corresponding to amorphous, polycrystalline, and single crystal. An abrupt jump in diffusivity, by a factor of about three, occurs at a temperature between 580 °C and 590 °C, consistent with the amorphous-polycrystalline transition temperature revealed in the XRD results (Sec. III. A). However, the diffusivity of the polycrystalline films is only one eighth that of the single-crystal value. There also appears to be an increase of about 50% in film diffusivity within the polycrystalline region at the highest deposition temperature 630 °C.

IV. DISCUSSION

We have measured the thermal diffusivity of LPCVD silicon thin films with fundamentally different microstructures, using a thermal wave technique. Specifically, we have demonstrated large differences in thermal diffusivity between the amorphous, polycrystalline and single-crystal states. These microstructural states are governed by the film processing conditions, specifically deposition temperature. Whereas a microstructural dependence of thermal properties has been demonstrated in other thin film systems,[8,11,14,24] studies on silicon films have not been systematically documented.

The essential details of our results are contained in Fig. 7. Consider first the amorphous state, below deposition temperature 580 °C. The relatively low diffusivity is due to the atomic disorder, corresponding to a small phonon mean free path.[25] A rough estimate of average phonon mean free path can be made on the basis of the kinetic expression for thermal conductivity[25] and Eq. (1),

$$\alpha = vl/3 , \qquad (2)$$

where v is the speed of sound and l is the average phonon mean free path. Based upon the experimental data and Eq. (2), the deduced average mean free path for single-crystal silicon is about 100 nm, but that of amorphous silicon is only about 3 nm. The thermal conductivity $\kappa = 4.80 \pm 0.5\ \mathrm{Wm^{-1}\,K^{-1}}$ evaluated from our diffusivity measurements compares with a "film conductivity" $5.88\ \mathrm{Wm^{-1}\,K^{-1}}$ deduced from measurements on comparatively thin amorphous silicon films by Kuo *et al.* using photothermal interferometry.[26] Those authors noted a systematic increase in "effective conductivity" ($1.14-3.43\ \mathrm{Wm^{-1}\,K^{-1}}$) with increasing film thickness (0.25–1.75 μm). They attributed this increase to a film/substrate "interface resistance". We note from Fig. 7 that the data within the amorphous range are independent of deposition temperature within the experimental scatter. As these data were obtained on specimens with different thicknesses, ranging from 2.0 to 3.6 μm (Table I), this result implies the absence of any thickness effect on the diffusivities of this set of films. This may be a consequence of the larger film thicknesses used in our experiments; any interfacial resistance would be expected to have less significant effect on thicker films than on thinner ones.

The more interesting results are obtained in the polycrystal region of Fig. 7. The substantially greater diffusivity relative to that in the amorphous region (a

factor of three or more) is a reflection of the longer mean free path associated with the ordered crystalline state.[25] However, this diffusivity is still nearly an order of magnitude less than the single-crystal value, implying the existence of extrinsic phonon scattering centers. Such scattering centers are attributable to microstructural features in the films, e.g., columnar grain boundaries and defects. The fine columnar grain structure in Fig. 4 indicates a high density of grain boundaries extending across the film section, most likely with segregated extra defects.[8,27–29] Boundary scattering can occur from phonon reflection at grain boundaries.[30] When the grain size is comparable to the phonon mean free path, this scattering can be sufficiently large to lower the thermal conductivity. Such an effect on thermal conduction has been observed in other polycrystalline materials at room temperature, such as bulk CVD β–SiC.[31] Defects, such as clusters of foreign or disordered atoms, strain fields surrounding dislocations, etc., will serve as additional scattering sources, further impeding thermal transport.[8,30] Scattering at grain boundaries would be especially effective in reducing the lateral thermal conductivity of the films with columnar structures as the lateral heat conduction is orthogonal to the columnar grain boundaries. Figure 4 also shows that large grains, which are twinned but impurity-free (Sect. III. B), interrupt the fine grain structure. This feature is very similar to that reported by Watanade *et al.* for silicon films deposited under similar conditions[23]; the mechanism of the large grain formation was attributed to a high mobility of surface atoms. These large grains are expected to be better thermal conductors than the fine columns, because little effect on phonon scattering may be expected from relatively low-disorder, clean twin boundaries[8] and because the size of the grains is larger than that of the fine grains by almost an order of magnitude, reducing scattering at grain boundaries. If the area fraction of large grains were to exceed some percolation threshold,[33] such that interconnectivity occurs between these large grains, the heat flow path would be "short-circuited", leading to an abrupt increase in conductivity. This may explain the high value of diffusivity for the specimen at 630 °C in Fig. 7, corresponding to a threshold area fraction somewhere near 0.36 (Table I).

It is interesting to compare our data on the polycrystalline films with some previous published values. Volklein and Baltes reported $\kappa = 29\ \mathrm{Wm^{-1}\,K^{-1}}$ for the out-of-plane thermal conductivity of *n*-type LPCVD polycrystalline silicon films,[34] higher than the value for the in-plane thermal conductivity $\kappa = 15–23\ \mathrm{Wm^{-1}\,K^{-1}}$ obtained in our study. Quantitative comparison is not feasible here since microstructural information for their films is not available. However, it is expected that the out-of-plane conductivity should be higher than in-plane conductivity for CVD films with columnar structures. Such an anisotropy of thermal conductivity has indeed been observed in columnar growth bulk polycrystalline silicon,[35] and in CVD diamond films.[8] The strong dependence of thermal conductivity on microstructural features implies that precautions have to be taken when applying any thermal data to a specific film system.

The present results provide thermal conductivity data of silicon thin films. More importantly, they indicate the important role of microstructure in determining the thermal conductivity. There are major effects in going from the amorphous to the polycrystalline states, and from the polycrystalline to the single-crystal states. In addition, within the polycrystalline region, grain size appears to be an additional factor, and warrants further study. We have also demonstrated the utility of thermal waves, specifically the "mirage" technique, as a nondestructive, noncontact, and sensitive means for obtaining critical thermal data for thin films.

ACKNOWLEDGMENTS

L. Wei acknowledges fruitful discussions with B. R. Lawn and P. K. Kuo. J. Xu and A. J. Streckl acknowledge the assistance of G. DeBrabander and J. T. Boyd with the deposition of the Si films. Funding was provided by the OIPM at NIST. Work at UC was supported in part by the SDIO/IST and monitored by ARO, under Grant No. DAAL03-92-0290.

REFERENCES

1. *Amorphous and Microcrystalline Semiconductor Devices, Vol. II: Materials and Device Physics*, edited by J. Kanicki (Artech House, Boston/London, 1992).
2. *Polysilicon Thin Films and Interfaces*, edited by T. Kamins, B. Raicu, and C. V. Thompson (Mater. Res. Soc. Symp. Proc. **182**, Pittsburgh, PA, 1990).
3. C. H. Mastrangelo and R. S. Muller, *Solid-State Sensor and Actuator Workshop*, IEEE Catalog No. 88TH0215-4, Hilton Head, SC, June 6–9, 1988, p. 43.
4. *Proceedings of the U.S.-Australia Joint Seminar on Enhanced Thermal Conductance in Microelectronics*, edited by M. I. Filk, K. E. Goodson, and A. Williams Melbourne, Australia (1992), p. 79.
5. J. A. Thornton, J. Vac. Sci. Technol. **11**, 666 (1974).
6. R. Messier, J. Vac. Sci. Technol. A **4**, 490 (1986).
7. J. C. Lambropoulous, S. D. Jacobs, S. J. Burns, L. Shaw-Klein, and S-S. Hwang, in *Thin-Film Heat Transfer–Properties and Processing*, edited by M. K. Alam *et al.* (ASME, New York, 1991), Series HTD, Vol. 184, p. 21.
8. J. E. Graebner, Diamond Films Technol. **3**, (2), 77 (1993).
9. P. Nath and K. L. Chopra, Thin Solid Films **18**, 29 (1973).
10. R. W. Powell, J. Sci. Instrum. **34**, 485 (1957).
11. J. R. Roger, F. Lepoutre, D. Fournier, and A. C. Boccara, Thin Solid Films **155**, 165 (1973).
12. A. Skumanich, H. Dersch, M. Fathallah, and N. M. Amer, Appl. Phys. A **43**, 297 (1987).
13. C. A. Paddok and G. L. Eesley, Appl. Phys. **60**, 285 (1986).
14. Z. L. Wu, P. K. Kuo, L. Wei, S. L. Gu, and R. L. Thomas, Thin Solid Films **236**, 191 (1993).

15. A. C. Boccara, D. Fournier, and J. Badoz, Appl. Phys. Lett. **36**, 130 (1980).
16. L. D. Favro, P. K. Kuo, and R. L. Thomas, in *Photoacoustic and Thermal Wave Phenomena in Semiconductors*, edited by A. Mandelis (Elsevier, New York, 1987).
17. A. J. Steckl, J. Xu, and H. C. Mogul, in *Silicon-Based Optoelectronic Materials*, edited by M. A. Tischler, R. T. Collins, M. L. W. Thewalt, and G. Abstreiter (Mater. Res. Soc. Symp. Proc. **298**, Pittsburgh, PA, 1993), p. 211.
18. T. R. Anthony, W. F. Banholzer, J. F. Fleischer, L. Wei, P. K. Kuo, R. L. Thomas, and R. W. Pryor, Phys. Rev. B **42**, 1104 (1990).
19. C. B. Reyes, J. Jaarinen, L. D. Favro, P. K. Kuo, and R. L. Thomas, in *Review of Progress in Quantitative Nondestructive Evaluation*, edited by D. O. Thompson and D. E. Chimenti (Plenum, New York, 1987), Vol. 6, p. 271.
20. L. Wei, Ph. D. Dissertation, Wayne State University, Detroit, MI (1992).
21. *CRC Handbook of Chemistry and Physics*, 6th ed., edited by R. C. Weast (Chemical Rubber Co., Cleveland, OH, 1986).
22. B. D. Cullity, *Elements of X-Ray Diffraction* (Addison-Wesley, Reading, MA, 1967).
23. *Handbook of Semiconductor Silicon Technology*, edited by W. C. O'Mara *et al.* (Noyes Publications, Park Ridge, NJ, 1990), p. 666.
24. J. C. Lambropoulos, N. R. Jolly, C. A. Amsden, S. E. Gilman, M. J. Sinicropi, D. Diakomihalis, and S. D. Jacobs, J. Appl Phys. **66** (9), 4230 (1989).
25. C. Kittel, *Introduction to Solid State Physics*, 6th ed. (John Wiley & Sons, Inc., New York, 1988).
26. B. S. W. Kuo, J. C. M. Li, and A. W. Schmid, Appl. Phys. A **55**, 289 (1992).
27. L. L. Kasmerski, in *Polysilicon Films and Interfaces*, edited by C. Y. Wong, C. V. Thompson, and K. N. Tu (Mater. Res. Soc. Symp. Proc. **106**, Pittsburgh, PA, 1988), p. 199.
28. A. V. Hetherington, C. J. H. Wort, and P. Southworth, J. Mater. Res. **5**, 1591 (1990).
29. J. L. Batstone, Philos. Mag. A **67** (1), 51 (1993).
30. P. G. Klemens, Thermochemica Acta **218**, 247 (1993).
31. A. K. Collins, M. A. Pickring, and R. L. Taylor, J. Appl. Phys. **68** (12), 6510 (1990).
32. H. Watanabe, A. Sakai, T. Tatsumi, and T. Niino, Solid State Technol. 29 (July, 1992).
33. D. Stauffer and A. Aharmony, *Introduction to Percolation Theory* (Taylor & Francis, London/Washington, DC, 1992).
34. F. Volklein and H. Baltes, J. Microelectromechanical Systems **1** (4), 193 (1992).
35. K. E. Bean, H. P. Hentzschel, and D. Colman, J. Appl. Phys. **40** 2358 (1969).